

ASSESSING STRUCTURAL TECHNOLOGY PERFORMANCE FOR THE HYBRID WING BODY THROUGH PROBABILISTIC WEIGHT ESTIMATION

Jason A. Corman and Dimitri Mavris

Aerospace Systems Design Laboratory, Georgia Institute of Technology, Atlanta, GA 30332

Keywords: *conceptual aircraft design, weight estimation, uncertainty propagation, composites*

Abstract

Structural technologies like the Pultruded Rod Stitched Efficient Unitized Structure (PRSEUS) concept are assessed by the reduction in weight that can be achieved by being incorporated in a vehicle design. Although development teams track technical performance with lower level metrics, the impacts of these characteristics and their uncertainty must be propagated to weight savings to assist decision makers in technology selection and maturation assessments. This paper presents an approach for probabilistic weight estimation to determine systems level PRSEUS performance using a direct, quantitative, and physics-based approach. Probability distributions of weight reduction for the NASA/Boeing N2A are shown along with sensitivities of structural weight to lower level sources of structural uncertainty.

1 Introduction

Decisions of whether or not to implement technologies in an aircraft program are made based on many factors, including performance, maturity, cost, customer perception, etc. These factors have one thing in common; they are all high level sources of information. If a structural technology is to earn its way on an aircraft, the technology development team must translate lower level performance metrics, like strains at design ultimate load or post-buckling stiffnesses, into higher vehicle level metrics, such as structural weight savings or fuel economy. Therefore, a functional re-

lationship is required that propagates lower level performance metrics into terms in which decision makers are most comfortable.

The need for performance metrics at a high level poses a challenge for technologies like the Pultruded Rod Stitched Efficient Unitized Structure (PRSEUS) concept, which was designed for the hybrid wing body (HWB) configuration. There is little to no statistical weight information for the HWB concept since it has never been in production, unlike its tube-and-wing counterpart. Therefore, conceptual phase weight estimates rely on more direct, physics-based approaches, as developed by Bradley[3], Gern[4], and Laughlin[7]. These approaches determine weight of the primary structure and scale it to include the impact of secondary structure, systems connections, and other structure not captured in the model. This scaling process is performed because little is known of the detailed structure and load cases that size that structure in the early design phases. The process is also representative of the inherent uncertainty in the conceptual phase of design, and since PRSEUS weight performance assessments must be made with only conceptual phase knowledge of the HWB, it is important to consider the uncertainty of these weight estimates.

Uncertainty quantification is also important for the technology development process itself. Technology maturity is commonly reported on the Technology Readiness Level (TRL) scale.[8] As computational analyses and physical experiments are performed for the technology, its

knowledge base increases and it climbs the metaphorical rungs of the TRL scale. This technical progression is synonymous with reduction of uncertainty, further motivating a quantifiable and traceable approach of propagating uncertainty from the technology level to the vehicle level.

This paper presents this type of probabilistic assessment for weight reduction performance of the PRSEUS technology. A first-order uncertainty propagation approach is implemented for the NASA/Boeing N2A HWB configuration, which contains an internal structure designed for passenger cabin pressurization. Rather than considering all conceptual phase uncertainties, only a few sources from PRSEUS and other traditional composites are modeled in order to isolate their impacts. Results that are shown include probabilistic distributions for structural weight in multiple sections of the N2A, along with sensitivities of structural weights to the sources of uncertainty that are considered.

2 Pultruded Rod Stitched Efficient Unitized Structure (PRSEUS)

The PRSEUS concept was developed to overcome some of the structural challenges associated with the combined loading condition of the HWB centerbody. Because the centerbody must act as a lifting surface as well as contain the pressurized passenger cabin, PRSEUS was proposed as a lightweight solution with stiffness and strength properties required for the centerbody loads. This section highlights some PRSEUS design characteristics and lower level performance attributes, explains how the systems design process is different with PRSEUS than traditional composites, and presents examples of structural uncertainties associated with this technology.

2.1 Design and Performance Attributes

PRSEUS achieves an expected weight reduction with a number of its attributes. First, the unitization of the structure reduces the need for fasteners and connectors typically required for stiffener assembly, and since the rod stringer and frame stiff-

eners are integrated, the continuous load paths decrease the stress concentrations in these connection points.[10] Stitching the stiffeners to the skin also allows for the arrestment of damage propagation, similar to the manner in which aluminum construction of conventional aircraft arrests damage. Additionally, the predominantly 0-degree fibers in the cured composite stringer rod allow for beneficial stiffness properties in the axial direction of the centerbody.[11] Finally, PRSEUS is able to carry significant load after the skin locally buckles between stiffeners, no longer making this a constraining failure mode for design.[13]

2.2 Damage Tolerant Design Philosophy

Damage arresting properties of PRSEUS allow for design with a different philosophy compared to traditional composites. Since traditional composite construction lacks a mechanism to arrest damage growth, the structure must be conservatively in accordance with a safe-life philosophy or redundant structure must be added. This prevents local damage, especially due to fatigue, from propagating and producing catastrophic failures during flight. However, it is assumed that cracks will be arrested at the PRSEUS stitch lines. Therefore, a fail-safe design philosophy can be taken with this damage tolerant PRSEUS configuration, increasing the design allowables relative to traditional composites.[2]

2.3 Structural Uncertainties

There are sources of uncertainty that affect the design and development process of PRSEUS and its impact on weight savings. Many of these uncertainties are common across traditional composite structures as well. Imperfections in the fabrication and curing process can cause variation in density, thickness, and curvature of the panels. While density has a direct impact on weight, the other parameters could require structural shimming during assembly as a corrective measure, further adding weight. Similarly, flaws, imperfections, and the need to maintain and repair these instances of damage introduce uncertainty for PRSEUS weight. Other sources of un-

certainty include resin voids, misaligned laminate plies, and non-visible damage that can occur to the laminates during fabrication. These factors can degrade structural performance, and these uncertainties must be considered in the design process to reduce the risk of an undersized structure that is not reliable in the presence of these uncertainties.

3 Approach and Case Study for Probabilistic Weight Estimation

A first-order, computationally efficient approach is presented in this section which probabilistically estimates weight savings of the PRSEUS technology compared to traditional composites. Both structural concepts are applied to a baseline HWB vehicle.

3.1 Baseline Aircraft

The N2A HWB configuration was used for this study and is a derivative of the SAX-40 vehicle, developed as part of the Massachusetts Institute of Technology Silent Aircraft Initiative (SAI).[12] This configuration has two podded engines mounted at the rear centerbody section with horizontal stabilizers on each side providing noise shielding. The N2A was originally designed as a cargo freighter for a 6,000-nm range with a mission profile typical of a transport aircraft. Other requirements included a 103,000 pound payload weight, a minimal initial cruise altitude of 35,000 ft, a cruise Mach number of 0.8, and a maximum field length of 10,000 ft. The internal structure, shown in Fig. 1, was generated using the parametric weight estimation environment developed by Laughlin[7] and is consistent with original drawings[5] and typical HWB passenger cabin layouts[9].

3.2 Weight Estimation Environment

The computational weight estimation environment used in this study was developed by Trevor Laughlin to parametrically assess structural weight in the conceptual design phase for the HWB. It contains a multidisciplinary analysis routine with aerodynamics and structures tools to

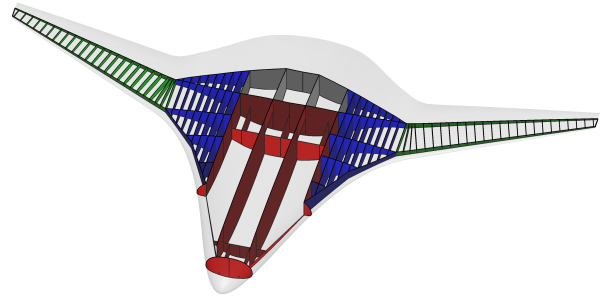


Fig. 1 Internal layout of the primary structure for the N2A

generate loads for the aircraft and apply them to the structure. This is followed by a single objective optimization routine within the structural code Hypersizer to size the structure for minimum weight. A detailed description of the functionality of this environment can be found in the following references[6, 7]; however, the process is briefly described in this section.

3.2.1 Geometry

Although this environment enables parametric investigation of the aircraft outer mold line (OML), this study was performed solely for the N2A baseline vehicle. The environment also allows for generation of an initial centerbody layout determined by passenger class using the ‘home-plate’ method in the NASA conceptual design tool, FLOPS.[9] However, since the OML for the N2A cargo transport was already defined, the dimensions for the centerbody passenger cabin were retrofitted for the geometry. Engines and horizontal stabilizers were not modeled for this study.

3.2.2 Structure

Internal structure for the N2A was generated using geometric relationships built into the weight estimation environment, and this structure can be seen in Fig. 1. These relationships enforce global load path continuity, especially from outboard wing bending and shear loads to the centerbody. The axial location of the rear spar of the outboard wing aligns with the rear bulkhead centerbody cabin, and a cargo bay bulkhead is also

placed at the x-location corresponding to the outboard wing front spar. These bulkheads bound the main landing gear bay. Only the primary load-bearing structure was included in the structural design, and therefore, the leading and trailing edges were not modeled for the trapezoidal and outboard wings.

The finite element model (FEM) created from this structural layout was built with shell elements for all skin, spar, rib, bay wall, and bulkhead components, and beam elements were used for spar, bulkhead, and bay wall caps. Elements were defined with a 12-inch mesh resolution, which was shown to be sufficiently converged for analysis with this environment.[6] All stiffened skin and sandwich structure were modeled with equivalent properties that were ‘smeared’ to shell elements, and therefore, no stiffeners were modeled discretely. Shear clips were not included in the FEM, and shell elements of the ribs were connected directly to the skin and spars, inducing a slight bending moment within the shear web. Although this can be considered a source of error in the model, it compensates for the small loads transmitted to the ribs by the limited number of loads cases that were included in the environment, which will be explained in the next subsection. This ensures the ribs are not undersized, and this overall approach is consistent with conceptual level structural models.

Weight reduction in this case study was determined by comparing PRSEUS structure to traditional composites, and the following descriptions explain how the structural concepts were applied to each section of the HWB.

Centerbody

A three-bay centerbody section was used for this configuration. PRSEUS was applied to all centerbody surfaces except intermediate bay walls (unstiffened sandwich structure), and the traditional structural counterpart for the case study was a 0-degree and 90-degree grid stiffened composite sandwich structure. Blade-stiffened composites were used for comparison on the landing gear bays and rear centerbody bulkheads. Constant stiffener spacing was enforced as a constraint,

an example of the connectivity Hypersizer allows to low-level composite design. Frame spacing was also required to be a multiple of the stringer spacing to simulate the transmission of loads more directly from the skin surface stiffeners to bay wall and bulkhead stiffeners.

Trapezoidal Wing

This inboard portion of the wing is a rib and spar arrangement in which load path continuity is enforced by joining each span-directed spar with a rib at the leading edge spar, as shown in Fig. 1. Each of these components is stiffened in the vertical direction with horizontal stiffening support nearest the thick centerbody section and adjacent to the landing gear. PRSEUS was applied to all surfaces in the trap wing for the trade study, where the frames did not include a foam core. Instead, the frames were used to simulate intercostals and aligned to the constant rib spacing to supply an attachment point for the shear web. This was not directly represented in the model due to property smearing to the shell elements, but it represents the logic behind the configuration to avoid any foam and fuel interaction. PRSEUS was compared to traditional blade-stiffened composites for the trapezoidal wing.

Outboard Wing

A conventional wing rib and spar arrangement was given to the outboard wing as well. Front and rear spars were located at 12% and 60% chord, respectively, and a constant rib spacing of 36 inches was used. The same logic was used in the outboard wing as the trap wing to compare PRSEUS to blade-stiffened composites, and the primary stiffener direction for the upper and lower skins was parallel to the rear spar.

3.2.3 Loads

A limited number of load cases was used in this study to size the structure, consistent with most critical loading conditions in the Phase 1 sizing study for PRSEUS[10] and the trade study performed by Gern[4]. These loading conditions are

defined as follows.

+2.5g Maneuver

A symmetric pull-up maneuver was executed at maximum takeoff weight (MTOW) with inertial relief from full fuel tanks on the wing.

-1.0g Maneuver

A symmetric pull-down maneuver was executed at MTOW, coupled with the inertial load of full fuel tanks.

2P Over-Pressure

The maximum pressure differential defined by FAR regulations is 9.2 psi. Design ultimate load for this load case is twice that pressure differential, but the vehicle does not need to sustain this pressure during flight.

2g Taxi Bump

While the fuel tanks are full, this load case applies a 2-g downward inertial load on all mass, including payload, fuel, and structural mass, which is reacted by the landing gear.

Aerodynamic loads for the maneuver cases were generated using PMARC, a panel method from NASA Ames Research Center, and applied to the structural mesh using an interpolating method.

3.2.4 Structural Sizing

All structural sizing was performed in Hypersizer Version 6.2. The routine within Hypersizer to minimize weight is a discrete and brute force approach. For each sizing group, a complete list of candidate designs is generated based on lower level structural design variables, their limits, and their desired number of permutations. These potential designs are then sorted from smallest to largest unit weight, and the sizing routine analyzes the designs in this order until all minimum margins of safety are exceeded. PRSEUS post-buckling performance was represented in Hypersizer by allowing negative margins of safety for local buckling between frames and stringers.

For this case study, a small set of knockdown factors was applied to traditional composite concepts to represent the difference between design philosophies with PRSEUS and traditional composites. They also cover relative difference in

Table 1 Knockdown factors on laminate properties for traditional composites

Knockdown	Value	Applied to
Non-damage tolerant	0.667	ϵ_{allow}
	0.8	σ_{allow}
Non-unitization	0.95	Equivalent E, G
	0.95	σ_{allow}
	0.95	ϵ_{allow}

allowables between the stitched PRSEUS structure and non-unitized composites that require fasteners for construction.[10] These factors can be seen in Table 1.

Calibration was performed with the weight estimation environment to scale the weight of the primary structure to total structural weight. A Boeing technical report by Kawai, which used the ‘EXTended Trailing Edge’ version the N2A, or N2A-EXTE, lists a breakdown of structural weight of the vehicle.[5] This configuration increases the length of the aft centerbody section by approximately 13-ft for engine integration and noise shielding compared to the baseline N2A; therefore, the weight stated in the report for the rear centerbody section was reduced by 20% before calibration. The report also mentioned that an in-house methodology was used, which analyzed advanced composite structure for weight predictions. A 10% increase in weight was applied for these centerbody and wing calibration points to represent the performance of traditional rather than advanced composites, consistent with the Phase 1 PRSEUS report.[10]

3.3 Uncertainty Propagation

The brute force sizing approach in Hypersizer requires a significant amount of computational time for design studies including PRSEUS, because a large number of low-level design variables exists for the structural technology. Therefore, a first-order linear expansion method, based on the work of Arras[1], was used to propagate structural uncertainties to vehicle level weight metrics. This approach, in terms of the case study variables, can be seen graphically in one dimension in Fig. 2, where W is a generic structural weight

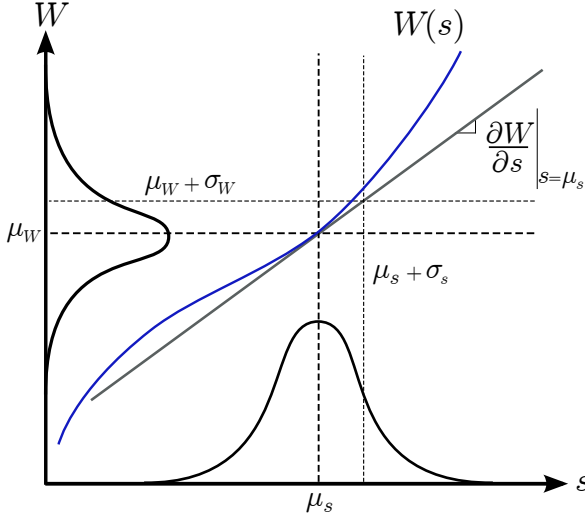


Fig. 2 Linear expansion concept for uncertainty propagation in one dimension

and s is a source of uncertainty. Assuming $W(s)$ is relatively linear in the region of the uncertain variable mean, μ_s , which is also the optimized configuration without uncertainty, then the projection of $\mu_s + \sigma_s$ on the linear weight function, with a slope of $\left. \frac{\partial W}{\partial s} \right|_{s=\mu_s}$, provides a good estimate of $\mu_W + \sigma_W$.

To expand this formulation to multiple uncertain variables, $s_i \in \mathbf{s}$, a first order Taylor series expansion can be defined as:

$$W = W(\mu_{s_1}, \mu_{s_2}, \dots, \mu_{s_n}) + \sum_{i=1}^n \frac{\partial W}{\partial s_i}(\mu_{s_1}, \mu_{s_2}, \dots, \mu_{s_n})(s_i - \mu_{s_i}) \quad (1)$$

In order to obtain the distribution for weight based on multiple sources of uncertainty, the variance can be found from this expansion with:

$$\sigma_W^2 = \sum_{i=1}^n \left(\frac{\partial W}{\partial s_i} \right)^2 \sigma_{s_i}^2 \quad (2)$$

where $\left. \frac{\partial W}{\partial s_i} \right|_{s_i=\mu_{s_i}}$ is evaluated at all μ_{s_i} and $\sigma_{s_i}^2$ is the variance of each uncertainty source, s_i . By using these equations, it is assumed that each of the sources of uncertainty is normally distributed and there is no correlation between any s_i . These assumptions are important, especially for composite structures in which there are many variables that could be affected by uncertainty. As more

uncertain variables are considered, the likelihood of interdependence increases, especially for manufacturing and fabrication uncertainties. For this study, a small number of uncertain variables was considered and the assumption of independence introduces little error for the variables chosen.

3.4 Test Case Parameters

Although stiffener spacing was held constant for PRSEUS and the other structural configurations, as detailed in Sec. 3.2.2, there were many other design variables the optimizer had control of for structural sizing, and they are listed in Table 2.

The five sources of uncertainty for this case study can be found in Table 3. These sources represent uncertainty that should be planned for in the conceptual design process, even though some are more linked to the fabrication process. For instance, composite laminate density has a direct physical connection to weight and varies due to the materials and processes used during fabrication. When an aircraft is built, its weight is a single deterministic value regardless of the difference between actual and predicted values of these densities, or other fabrication variations like thicknesses, laminate ply orientations, etc. However, by accounting for this variation early in the design process, the chances of meeting regulatory requirements for the vehicle are increased, avoiding costly redesign in later development and implementation phases.

The other uncertain variables listed in Table 3 have a more indirect relationship with physical weight, but are directly related to constraints in the design process. Material properties like stress and strain allowables affect the structural geometry constrained by strength- and stability-based failure modes. This geometry, along with mate-

Table 4 Structural weight metrics for the case study

Description	Symbol	$F_{s,i}$
Centerbody	W_{cb}	1.51
Rear Centerbody	W_{rcb}	1.8
Outboard Wing	W_{ow}	1.49
Trapezoidal Wing	W_{tw}	1.49
Total	W_{total}	—

Table 2 Structural design variables controlled in sizing routine

Structural Concept	Design Variable (x_i)
PRSEUS:	Thickness: Skin, Stringer Web, Frame Web, Foam Core Tear Strap, Frame Cap Height: Stringer, Frame Diameter: Rod
Blade-Stiffened Skin:	Thickness: Skin, Stringer Web Height: Stringer
Sandwich Structure:	Thickness: Top Skin, Bottom Skin, Stiffener Webs (0° and 90°) Height: Stiffener Webs (0° and 90°)

Table 3 Sources of structural uncertainty

Description	μ_s	σ_s
Composite Laminate Density, ρ_ℓ (lb/in^3)	0.057	0.002 (3.5%)
Change in Stress/Strain Allowables, $\Delta\sigma_a$ & $\Delta\varepsilon_a$ (%)	0.0	2.0
Change in Laminate Ply Angles, $\Delta\phi_{ply}$ (deg.)	0.0	2.0
Change in Fiber Stiffness, ΔE_f & ΔG_f (%)	0.0	2.0
Change in Calibration Factor, Δk_{scale} (%)	0.0	2.0

rial densities, defines the structural weight. For calibration factors, uncertainty can be introduced by choosing an inappropriate functional relationship of the calibration variable – in this case, a scale factor on primary structural weight. It can also be introduced if the calibration point is not considered a complete ‘truth model.’ For example, the weight values to which this environment was calibrated[5] were generated with a proprietary computational model and do not represent an as-built configuration. Therefore, an inherent uncertainty exists in these values if the goal of this environment is to predict ‘actual’ physical weight, and that is why calibration factors are included in this case study.

Since uncertainties are applied across multiple values for the same variable, e.g. allowables for both stresses and strains, the representative uncertainties are listed as percentages in Table 3. The weight metrics of interest for the N2A are shown in Table 4, along with nominal values for factors used to scale the weight of the primary structure to total structure. These scale factors were also used as the mechanism for model calibration, and were considered the source of uncertainty described in the previous paragraph.

3.5 Assumptions and Limitations

The approach presented in this section has its limitations. Since normality in uncertainty distributions must be assumed, a limited number of uncertain variables was investigated. Characterization of the sources of uncertainty was outside the scope of this project, so nominal distributions were chosen to highlight the uncertainty propagation technique. A degree of accuracy is maintained under the assumption of functional linearity for this propagation method, so long as the relationship is linear within the bounds of the uncertain variable distribution. The variation in weights shown in the next section is simply due to the sources of uncertainty considered in the study and is not an all-encompassing estimate of uncertainty in the conceptual design process. As the weight estimation environment is concerned, some weight savings opportunities for each structural configuration may be lost because of the discrete nature of the sizing process in HyperSizer. Further, including secondary structure in the finite element model would decrease the uncertainty in scale factors.

4 Results

By applying the approach described in the previous section, initial weight reduction performance assessments for PRSEUS with structural uncertainties is shown in this section.

4.1 Structural Weights

The aggregate impact of all sources of structural uncertainties is shown in this subsection. Through propagation with the first-order method, structural weight distributions for various sections of the N2A are shown for the two structural concepts in Fig. 3. The weight distributions are shown on a reverse x-axis to highlight the subtraction of distributions of the baseline configuration (black) by the PRSEUS configuration (blue). The resulting weight reduction distribution is shown on the right side in red for each metric. Comparing these normal distributions is done by subtracting mean values and adding variances, as shown in Eq. 3 and 4, respectively:

$$\mu_{\Delta W} = \mu_{W_b} - \mu_{W_p} \quad (3)$$

$$\sigma_{\Delta W}^2 = \sigma_{W_b}^2 + \sigma_{W_p}^2 \quad (4)$$

where W_b represents the weight of the baseline HWB and W_p represents the weight of the PRSEUS-enabled HWB. This trend can be seen from Fig. 3, in which the spread of the resultant weight savings distribution (red) is larger than each of the component distributions. One anomaly that can be seen in this figure is the structural weight increase in the trapezoidal wing (W_{tw}) when PRSEUS is used as the structural concept in this region. There are two potential explanations for this. First, the discretization scheme in Hypersizer did not allow for a truly optimal configuration to be found for PRSEUS, but it may have for traditional composites. Second, the upper limit for spar thickness was not large enough at the inboard section so unnecessary weight was added to the configuration by auxiliary means, e.g. bulky stiffeners. The latter is supported by larger variation of weight in the outboard wing, as seen in Table 5. This highlights the importance of setting reasonable variable bounds in the structural sizing process.

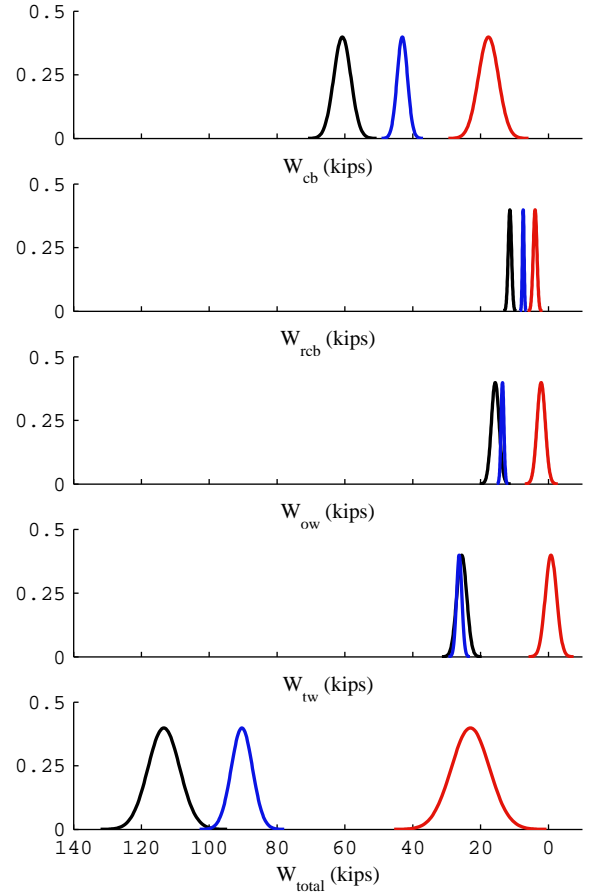


Fig. 3 Uncertainty distribution of PRSEUS weight savings is shown in red, as the difference between the baseline weight distribution (black) and PRSEUS weight distribution (blue).

Weight savings distributions for all metrics are listed in Table 5.

4.2 Weight Sensitivities to Sources of Uncertainty

The spread of the aggregate distributions in the previous subsection are the result of multiple variance effects as defined by Eq. 2. A mapping of the uncertainty of total structural weight

Table 5 Distributions of weight changes with PRSEUS for N2A

Section	$\mu_{\Delta W}$ (lb)	$\sigma_{\Delta W}$ (lb)
ΔW_{cb}	-17,688 (-29.1%)	2,952 (4.9%)
ΔW_{rcb}	-3,939 (-34.6%)	545 (4.8%)
ΔW_{ow}	-2,134 (-13.6%)	1,218 (7.8%)
ΔW_{tw}	+749 (+2.9%)	1,662 (6.5%)
ΔW_{total}	-23,009 (-20.3%)	5,615 (5.0%)

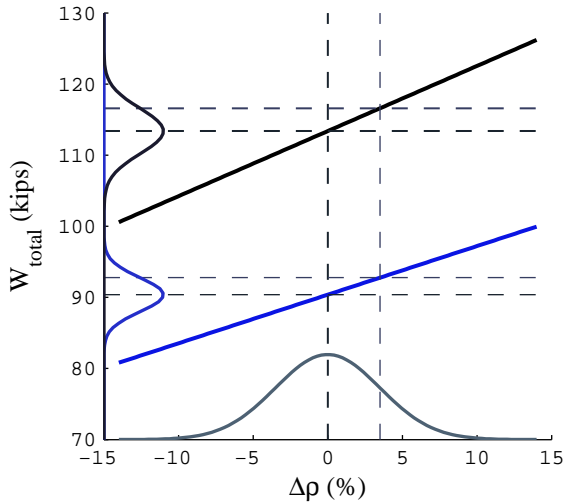


Fig. 4 The mapping of percentage change in density uncertainty is shown to uncertainty in total structural weight for the baseline and PRSEUS configurations.

due to material density can be found in Fig. 4. Uncertainty is mapped to both the baseline and PRSEUS N2A configurations, which are drawn to the same scale. It is shown in this figure, due to the larger slope of the baseline configuration, that uncertainty in density will propagate to a larger amount of uncertainty in the structural weight of the baseline than that of the PRSEUS design.

Non-graphical data for more mappings is found in Table 6. This table shows the effects of two sources of uncertainty, laminate density (ρ) and stress/strain allowables (σ_a and ϵ_a). The top two rows represent effects on the baseline, designated with the subscript b , while the bottom two rows show effects for the PRSEUS-enabled N2A, designated with the subscript p . Columns in Table 6 represent the slope or sensitivity of the weight function to each source of uncertainty, $\frac{\partial W}{\partial s}$, and the variance of weight due to each source, σ_W , for the centerbody, rear centerbody, outboard wing, trap wing, and total vehicle, respectively. There are two instances of a reduction in weight when adverse values for uncertainties are applied, shown with negative slopes. This is most likely a result of course discretization on structural design variables in Hypersizer, and the brute force method uncovering weight opportunities with small changes in the uncertain variables.

5 Conclusions

Assessing weight savings for structural technologies is not a trivial process when performed probabilistically, especially for the HWB configuration. Since the baseline weight in this situation is also a probability distribution, this further increases the amount of uncertainty for the weight comparison. Traditional composites will likely have smaller distributions for structural uncertainties since they are more developed and it is probable they have already been in production. However, structural uncertainties for demonstration purposes in this case study were handled in the same manner across structural configurations since characterization was outside the scope of the project. This is reasonable for initial estimates since traditional composite weight for the HWB is determined under the same design process uncertainties as PRSEUS. Due to these considerations, structural weight reduction distributions have a large spread since variances are added when subtracting two normal distributions.

These insights were enabled by a quantitative approach to uncertainty propagation. Uncertainty propagation can be performed with more elegant methods to incorporate a larger number of uncertainty sources, so long as obstacles in the weight estimation environment are overcome and assumptions in the propagation process are applicable. It was shown that the structure built in the weight estimation environment was representative of a passenger HWB vehicle, and through structural modeling in Hypersizer, low-level design variables were connected to high level metrics. The control of these parameters also ensured structural configurations were representative of the actual structure before properties were ‘smeared’ to equivalent shells in the FEM. This approach, even with its limitations, was an adequate method for initial performance and uncertainty assessments as long as appropriate design and uncertain variables are considered.

The authors would like to graciously thank Dawn Jegley and Alex Velicki for their guidance and insight with the PRSEUS concept as well as Trevor Laughlin for his efforts with the HWB weight estimation environment.

Table 6 Sensitivities of weights to sources of uncertainty and standard deviation of weight components

s	$\frac{\partial W_{cb}}{\partial s}$	$\sigma_{W_{cb}}$	$\frac{\partial W_{rcb}}{\partial s}$	$\sigma_{W_{rcb}}$	$\frac{\partial W_{ow}}{\partial s}$	$\sigma_{W_{ow}}$	$\frac{\partial W_{tw}}{\partial s}$	$\sigma_{W_{tw}}$	$\frac{\partial W_{total}}{\partial s}$	$\sigma_{W_{total}}$
ρ_b	301	1,058	94	328	215	756	303	1,065	915	3,212
$\sigma_{a,b}$ & $\epsilon_{a,b}$	-301	602	29	58	356	712	402	803	487	975
ρ_p	304	1,069	44	156	115	403	220	771	683	2,339
$\sigma_{a,p}$ & $\epsilon_{a,p}$	314	629	-8	16	42	85	0	0	348	697

References

- [1] K. O. Arras. An introduction to error propagation: Derivation, meaning and examples of equation $c_y = f_x c_x f_x^t$. Technical report, Autonomous Systems Lab, Institute of Robotic Systems, Swiss Federal Institute of Technology Lausanne (EPFL-ASL-TR-90-01 R3), 1998.
- [2] A. C. Bergan, J. G. J. Bakuckas, A. E. Lovejoy, D. C. Jegley, J. Awerbuch, and T.-M. Tan. Assessment of damage containment features of a full-scale prseus fuselage panel through test and teardown. In *27th ASC Technical Conference*, 2012.
- [3] K. R. Bradley. A sizing methodology for the conceptual design of blended-wing-body transports. Technical report, NASA/CR-2004-213016, 2004.
- [4] F. H. Gern. Finite element based hwb centerbody structural optimization and weight prediction. In *53rd AIAA/ASME/ASCE/AHS/ASC Structures, Structural Dynamics and Materials Conference*, 2012.
- [5] R. Kawai. Acoustic prediction methodology and test validation for an efficient low-noise hybrid wing body subsonic transport. Technical report, NASA, 2011.
- [6] T. W. Laughlin. A parametric and physics-based approach to structural weight estimation of the hybrid wing body aircraft. Master's thesis, Georgia Institute of Technology, 2012.
- [7] T. W. Laughlin, J. A. Corman, and D. N. Mavris. A parametric and physics-based approach to structural weight estimation of the hybrid wing body aircraft. In *51st AIAA Aerospace Sciences Meeting including the New Horizons Forum and Aerospace Exposition*, 2013.
- [8] J. C. Mankins. Technology readiness levels: A white paper. Technical report, NASA Office of Space Access and Technology, 1995.
- [9] C. L. Nickol and L. A. McCullers. Hybrid wing body configuration system studies. In *47th AIAA Aerospace Sciences Meeting including The New Horizons Forum and Aerospace Exposition*, 2009.
- [10] A. Velicki. Damage arresting composites for shaped vehicles: Phase 1 final report. Technical report, NASA/CR-2009-215932, 2009.
- [11] A. Velicki, N. Yovanof, J. Baraja, K. Linton, V. Li, A. Hawley, P. Thrash, S. DeCoux, and R. Pickell. Damage arresting composites for shaped vehicles: Phase ii final report. Technical report, NASA/CR-2011-216880, 2011.
- [12] P. A. Weed. Hybrid wing-body aircraft noise and performance assessment. Master's thesis, Massachusetts Institute of Technology, 2010.
- [13] N. P. Yovanof and D. C. Jegley. Compressive behavior of frame-stiffened composite panels. In *52nd AIAA/ASME/ASCE/AHS/ASC Structures, Structural Dynamics and Materials Conference*, 2011.

Contact Author Email Address

mailto:jason.corman@gatech.edu

Copyright Statement

The authors confirm that they, and/or their company or organization, hold copyright on all of the original material included in this paper. The authors also confirm that they have obtained permission, from the copyright holder of any third party material included in this paper, to publish it as part of their paper. The authors confirm that they give permission, or have obtained permission from the copyright holder of this paper, for the publication and distribution of this paper as part of the ICAS 2014 proceedings or as individual off-prints from the proceedings.